Building a continuous attractor model of dMEC grid cells using conductance-based neurons

A Thesis

submitted to

Indian Institute of Science Education and Research Pune
in partial fulfillment of the requirements for the
BS-MS Dual Degree Programme

by

Akshay Nair

Indian Institute of Science Education and Research Pune
Dr. Homi Bhabha Road,
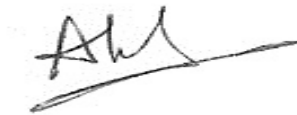Pashan, Pune 411008, INDIA.

June, 2020

Supervisor: Dr. Collins Assisi

© Akshay Nair 2020

Certificate

This is to certify that this dissertation entitled *Building a continuous attractor model of dMEC grid cells using conductance-based neurons* towards the partial fulfilment of the BS-MS dual degree programme at the Indian Institute of Science Education and Research, Pune represents study/work carried out by Akshay Nair at the Indian Institute of Science Education and Research under the supervision of Dr. Collins Assisi, Assistant Professor, Department of Biology, during the academic year 2019-2020.

Akshay Nair   Dr. Collins Assisi

Committee:

Dr. Collins Assisi

Dr. Pranay Goel

Declaration

I hereby declare that the matter embodied in the report entitled *Building a continuous attractor model of dMEC grid cells using conductance-based neurons* , are the results of the work carried out by me at the Department of Biology, Indian Institute of Science Education and Research, Pune, under the supervision of Dr. Collins Assisi and the same has not been submitted elsewhere for any other degree.

Akshay Nair   Dr. Collins Assisi

Abstract

The work done in this thesis attempts to model the grid cell network, pivotal in spatial navigation and awareness, using biologically realistic descriptions of neurons. While previous work on this system used rate-based models to simulate the activity of neurons, these models are not able to realistically represent the dynamics of neuronal behaviour. In this thesis, we use conductance-based models of stellate cells and fast-spiking interneurons to construct two types of networks built using a primitive MEC motif. These networks are able to show the formation and movement of an idealized bump of activity along a single dimension. The networks and the translation of the bump are able to show direction- as well as speed-tuning. Theta oscillations are shown to play a role in tunability and control of the system and may play a part in stabilzation of the temporal activity profile. The neuronal networks presented here provide the initial steps in making a full, biologically realistic, model of the grid cell network.

List of Figures

List of Tables

Acknowledgments

I would like to thank my supervisor Dr. Collins Assisi for giving me the opportunity to work on this project with him in his lab. His insight and guidance have been extremely helpful to me at every step of my project.

I would like to thank my TAC member Dr. Pranay Goel for providing valuable feedback and suggestions.

I would like to thank IISER Pune for providing assistance in the form of infrastructure and other technical support.

I would like to thank all the members of the Computational Neurobiology Lab. Their advice and the discussions we had were instrumental in this endeavour.

I would like to thank the other members of Let's Keep Thinking, Rahul, Palash, Prasanna, Simran, and Sunil for the intensely rewarding and thought-provoking band sessions we had throughout the years. The time spent with you has been one of the biggest highlights of my life here in IISER.

My sincerest gratitude to Sanjana, Aarcha, and Shomik for the wonderful times we spent together. Their constant support and encouragement is greatly appreciated throughout the course of my time at IISER Pune, and particularly my final year here.

Contents

Chapter 1

Introduction

Spatial navigation in animals is a complex problem. It entails the study of many different types of systems that take in many different kinds of sensory information. Various regions of the brain, like the hippocampus, are involved in different aspects of navigation and spatial perception. Many different neuronal cell types are involved in this activity. There are the place cells [O'Keefe, 1976] that fire when mice are at particular locations (or places), speed cells [Sargolini et al., 2006] that show varying firing rates as the mouse changes its speed of motion, head-direction cells [McNaughton et al., 2006, Hafting et al., 2005], the activity of which maintains an internal estimate of the direction the head of the mouse is facing, and grid cells [Hafting et al., 2005] whose activity maintains an internal estimate of the position of the mouse with respect to its surroundings. The navigation system uses external landmarks as well as idiothetic cues to help the mouse be cognizant of its position in the local environment. These cues help the animal to keep track of its environment even in darkness [McNaughton et al., 1996].

Grid cells in particular are a fascinating group. Each of these has several firing fields that are arranged as the vertices of a hexagonal lattice [Hafting et al., 2005]. Although the firing response of grid cells seems to be anchored to external landmarks, experiments have also showed that the grids exist and even persist in darkness. Thus, the mouse uses idiothetic as well as external cues to compute these grids and to traverse through them. The firing fields of different grid cells are skewed from each

other such that they tesselate local space. As the mouse moves in two dimensions, one can imagine that the neuronal activity moves across the population of grid cells correspondingly. This specific activity has lead to grid cells being implicated in dead-reckoning, the process of determining one's current position using knowledge of a previous position and idiothetic information such as velocity.
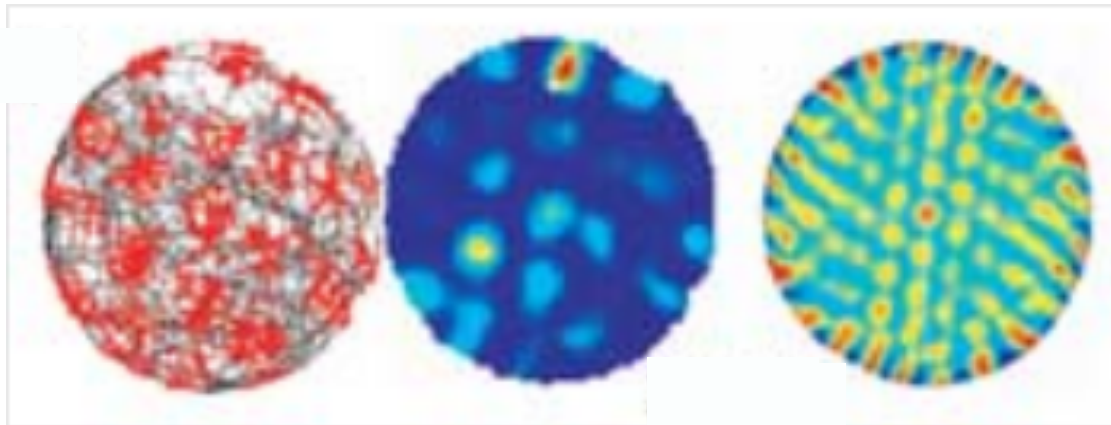

Figure 1.1: Activity of a single grid cell: as the mouse moved in a circular enclosure, its trajectory and locations where the grid cell fired were recorded. Left: trajectory is shown in black and grid cell firing locations in red. Center: rate map of the grid cell. Right: spatial autocorrelogram of the grid cell activity. From Figure 2c of [Hafting et al., 2005]

There have been several attempts to model the activity of the grid cell network [Giocomo et al., 2011, Burak and Fiete, 2009] and these models can broadly be classified into two types: the interference models and the attractor models [Zilli, 2012]. Only attractor models will be discussed here. The idea behind attractor models is that the activity of a population of neurons is constrained to one of many stable states. It is helpful to think of it as a manifold to which the motion of the state vector of the system is restricted. If the system finds itself in an unstable state, it quickly moves towards a stable one. Thus, in state space, there exists a manifold or an attractor that attracts the state of the system and it is free to move between stable states as each state is equally stable. Since this manifold is continuous rather than discrete, it can also be refered to as a continuous attractor network. Such attractor networks maintain that the special patterns of neuronal activity are emergent phenomena of the system, which come about as a result of asymmetrical connections between neurons. This asymmetry can be in the form of local or global inhibition, specificity of

neuronal response to different input types, and synaptic connections between neurons as well.

In an effort to understand the grid cell network in the mouse entorhinal cortex, [Burak and Fiete, 2009] modelled a sheet of neurons as a continuous attractor network. Neuronal activity was described in their model by the following equations:

$$\tau \frac{ds_i}{dt} + s_i = f\left[\sum_j W_{ij}s_j + B_i\right]$$

$$W_{ij} = W_0(\mathbf{x}_i - \mathbf{x}_j - l\hat{\mathbf{e}}_{\theta_j})$$

$$W_0(\mathbf{x}) = \mathbf{a}\mathbf{e}^{-\gamma|\mathbf{x}|^2} - \mathbf{e}^{-\beta|\mathbf{x}|^2}$$

where s_i is the synaptic activation of neuron i, W_{ij} is the synaptic weight from neuron j to neuron i, and B_i is the feedforward input to neuron i. Neuron j has a directional tuning specified by $\hat{\mathbf{e}}_{\theta_j}$ which is the unit vector in the direction θ_j. W_{ij} thus takes the form of a center-surround shape whose center is located not at neuron j itself but a distance l away from it along its tuned direction. This means that each neuron excites other neurons in a direction specified by its tuning.

While the model was able to exhibit characteristics similar to those shown by grid cells, the full range of behaviours that are exhibited by neurons cannot be modelled by a single equation. For instance, it does not take into account the ions that cross the cell membrane that are responsible for the changing membrane potential. The Hodgkin-Huxley model in contrast, uses 4 dynamical equations to specify a single neuron. Adding additional neurons involves the modelling of synapses which require additional equations and parameters as well. In order to address this gap between simple models and complex systems, we worked to come up with a model of the grid cell network activity using biologically realistic descriptions of neurons.

Various different cell types can be found in the MEC of which, the principal cell type is the stellate cell. These are cells that show some special characteristics. When they are slightly depolarized, they show small fluctuations in their membrane potential, called subthreshold oscillations [Alonso and Llinas, 1989, Alonso and Klink, 1993], and when released from hyperpolarization, they show rebound-spiking behaviour.

Aside from stellate cells, one can also find inhibitory interneurons in the MEC. These are present in close proximity to stellate cells; evidence suggests that the basic neuronal motif in the MEC consists of these two cell types. In accordance with this, we used conductance-based models of stellate cells ([Acker et al., 2003]) and fast-spiking interneurons ([Wang and Buzsaki, 1996]) to construct a network model of the grid cell network.

Due to the similarities of each grid cell's activity, as a mouse moves around in an enclosure, we can be content with a model in which the grid cells are topographically arranged. Such a model would disagree with the actual system as far as the positions of particular neurons are considered, but we hope that connecting topographically-arranged stellate cells, in a manner such that the network is able to show behaviours that the real system exhibits, will point towards similar connections between corresponding stellate cells in a non-topographic map. To that end, we do not discuss how such particular connectivities could come about over the course of development of the mouse brain. A similar approach is undertaken in other seminal works on the topic [Burak and Fiete, 2009].

The many bumps that appear across the sheet of neurons have a clear directionality to them. Three main axes are apparent as the arrangement is hexagonal. Traversing across any of the axes (or indeed, any straight line across the sheet) gives one an idea of the response of the system when constrained to a single dimension. In effect, a one-dimensional version of the model would consist of a line of neurons whose activity profile would manifest in the form of a bump of activity that was able to traverse across the cells. We attempted to construct a model that was capable of simulating this single-dimension behaviour in the hope that principles similar to ones that were employed in the one-dimensional model would be at play in the full model.

Chapter 2

Results

2.1 MEC motif
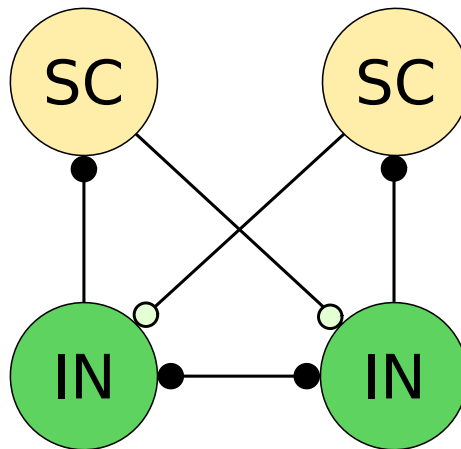
Figure 2.1: Prototype circuit used in [Neru and Assisi, 2019]. SC - Stellate cell, IN - Interneuron. Excitatory synapses are shown by light circles and inhibitory synapses by dark ones.

The primitive motif that we used was explored by [Neru and Assisi, 2019] (Figure 2.1). It is constituted of two stellate cells and two interneurons. The interneurons inhibit each other and a stellate cell each. Each stellate cell excites the interneuron that does not innervate it. Due to rebound-spiking in stellate cells, this simple circuit can exhibit a wide range of behaviour. In their paper, they discuss two modes that

(a) Autonomous Oscillator   (b) Bistable Switch

Figure 2.2: Firing in the primitive MEC motif. The top panels show the firing of stellate cells while the bottom panels show the same for interneurons. Values of current used: (a) SC input = -3 mA, IN input = 0.5 mA; (b) SC input = -3 mA, IN input = 1 mA
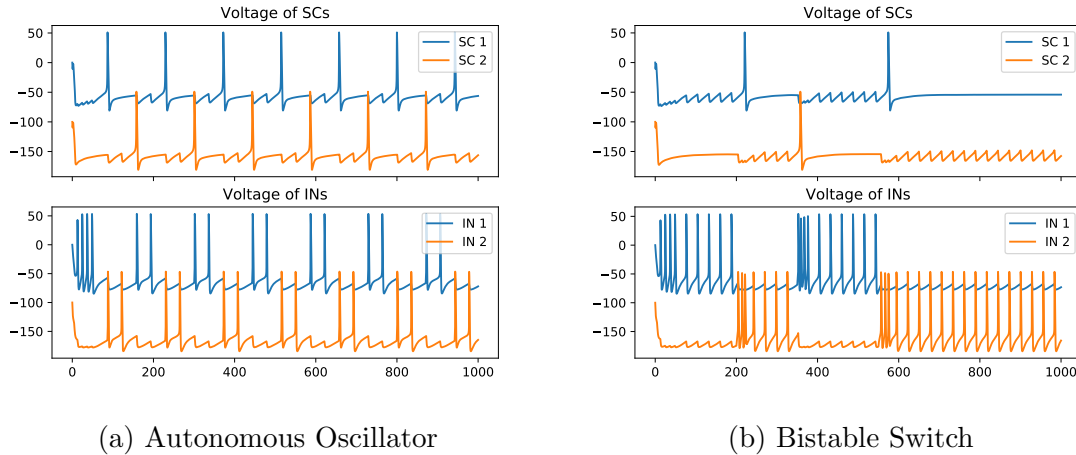
the network can operate in, which is determined by the current input given to the interneurons. These are:

1. Autonomous oscillator: When the interneurons are given a sufficiently weak input, the network activity oscillates between the two. At any point in time, one of the interneurons is active and its spikes inhibit a stellate cell. Due to the low current, the firing rate of the interneuron is low and so, the stellate cell is able to show rebound-spiking in between spikes of the interneuron. This excites the other interneuron, whose spiking then both inhibits the active interneuron and excites the other stellate cell. This change in activity occurs periodically and without external intervention, hence is autonomous.

2. Bistable switch: When the interneurons are given sufficiently strong input, one of them (winning the competition) shows spiking activity until a pulse of current is provided to the other interneuron. The previously inhibited interneuron then starts spiking and prevents the other interneuron from doing so. Each such shift in activity is marked by a spike in a stellate cell due to rebound-spiking: since it is released from inhibition, it is able to spike. The stellate cells do not show continuous spiking because of the high firing rate of the interneurons. The interneuron spikes occur faster than the membrane potential of the stellate cells

rises to its spiking threshold. The locus of activity in this mode does not shift until subsequent pulses are provided to interneurons. This mode is an example of a driven circuit as the network's activity changes only when external input is provided.

Due to the fact that stellate cell activity is the readout of our target system, we expanded upon the above motif and operated it in the oscillator regime to construct our first network.
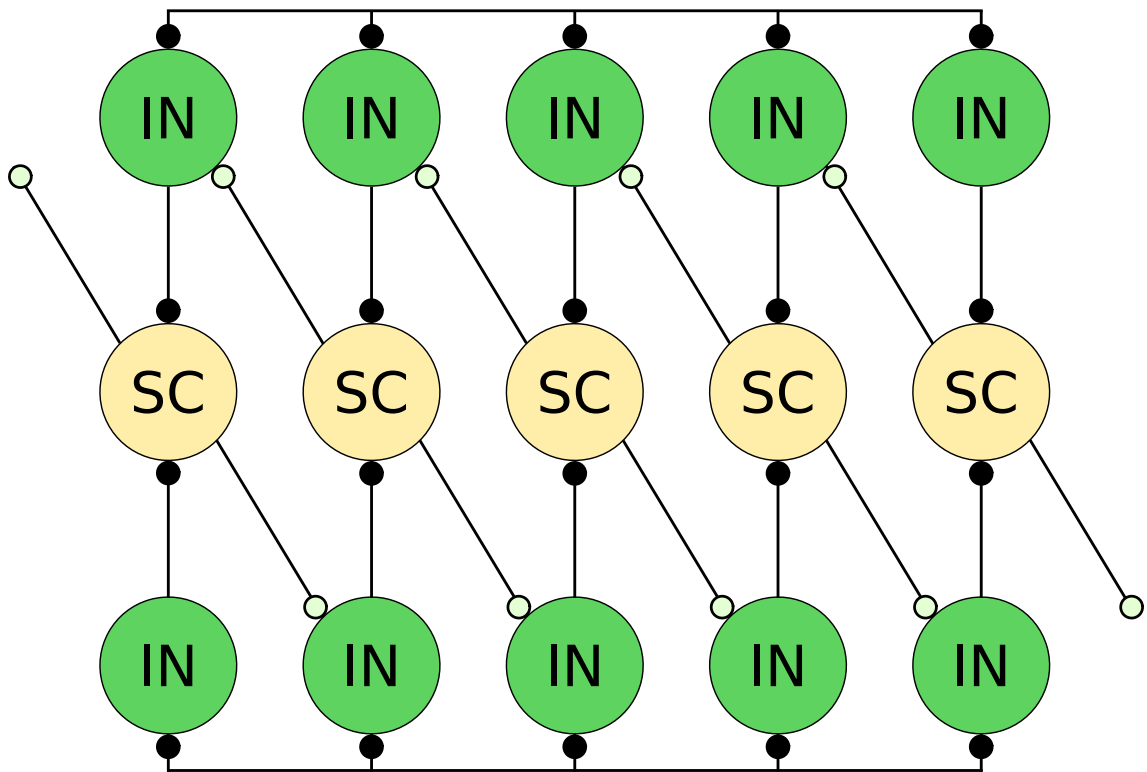
2.2 Network 1

Figure 2.3: Network 1. SC - Stellate cell, IN - Interneuron. The number of interneurons is doubled to allow the activity bump to show translations in both directions.

Chaining multiple units of the MEC motif and connecting the ends together to make a circular connection gave us our first foray into modelling the system (Figure

2.3). With this network, we were able to obtain an idealized bump which moved across the network. Each such spike provided the impetus for the next stellate cell in the sequence to fire; this mechanism of switching is the same as that in the autonomous oscilllator regime of the primitive circuit motif. This iteration of the model served as a proof of concept and showed that we were able to obtain and move an idealized bump across the network of cells. The size of this network could be increased simply by adding more neurons to the network. By manipulating the current input to the various cells, we were able to control whether the bump moved or stayed put. Two different activity profiles were seen:

1. Translatory phase : The bump of activity moves across the network. This is the situation where the mouse is moving along an axis. The bump is moved by exciting and inhibiting groups of interneurons, similar to in the primitive motif.

2. Stationary phase : The activity bump remains stationary, which is analogous to the mouse making no movement. This is done by inhibiting all the interneurons and exciting the currently firing stellate cell.

2.2.1   Direction tuning in Network 1

An additional ring of interneurons was added to Network 1 whose connections from stellate cells was in the opposite direction as before (Figure 2.3). This set of interneurons allowed the neurons in Network 1 to show translations of the bump in both directions. By making one group of interneurons more receptive to stellate cell spiking (and the other group less), we were able to control the direction of translation of the activity bump. This is done by providing a constant inhibitory current to one group to depress it, while the other remained excited. The group that is not inhibited is allowed to spike in response to the stellate cells and so, moves the bump along the direction specified by its connections. Figure 2.4 shows direction tuning in Network 1.
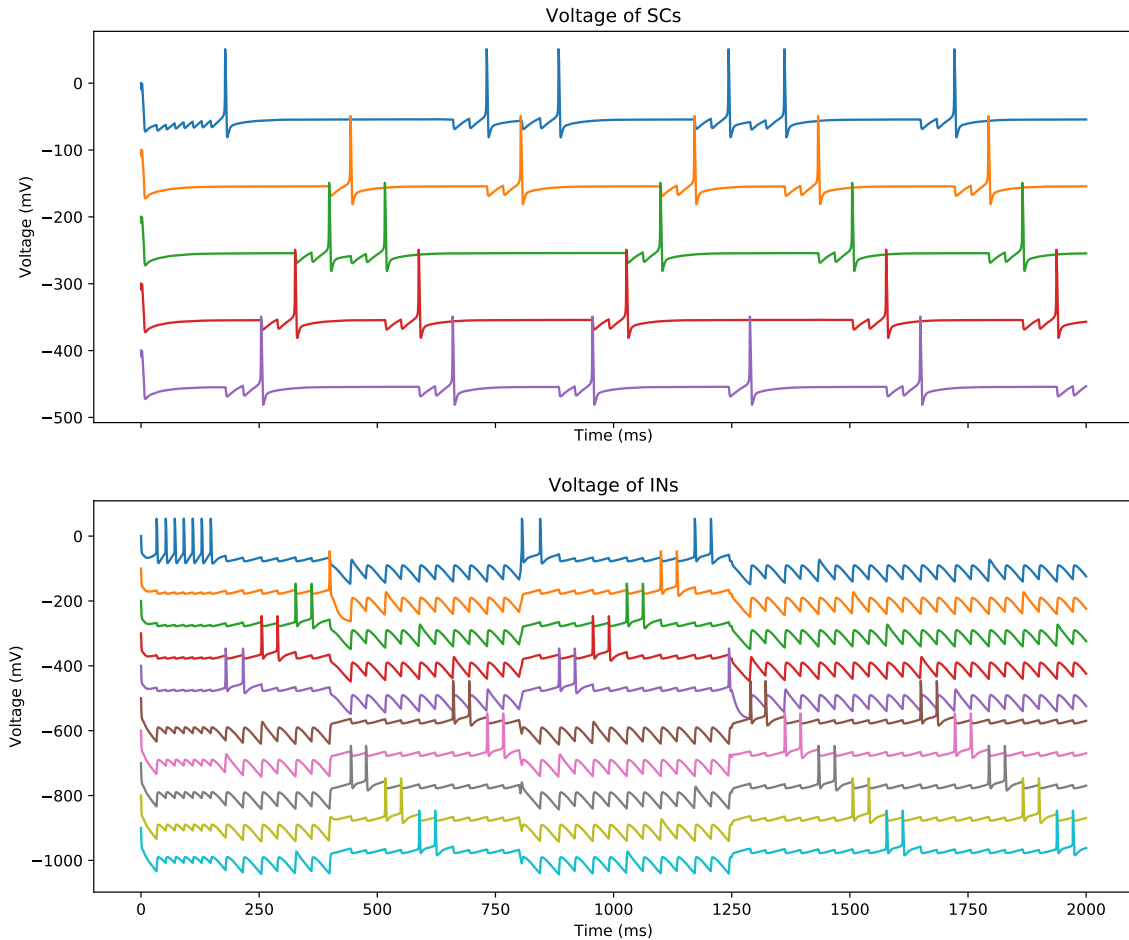
Figure 2.4: Direction tuning in Network 1. Top panel: Voltage traces of stellate cells (SCs) plotted against time. Bottom panel: Voltage traces of interneurons (INs) plotted against time. Current values used: SC input = -3 mA, IN input = 0.5 mA (for excited INs) and -10 mA (for inhibited INs)

2.3 Network 2

While Network 1 was able to show that a network of stellate cells and interneurons could move a single idealized bump, it had some drawbacks. First and foremost, the bump was idealized. The real system's activity bumps are measures of the grid cells' firing rates. At any point in the neuronal sheet, neurons being more active means they spike more often than those elsewhere. Thus, an activity bump should have neurons spiking faster than others. In Network 1, the bump consisted only of a singular neuron spike. A more realistic bump would have many spikes per neuron as well as more

Inhibitory connections to INs

Postsynaptic neuron index

	1	2	3	4	5
1	0	1	1	1	1
2	1	0	1	1	1
3	1	1	0	1	1
4	1	1	1	0	1
5	1	1	1	1	0

Presynaptic neuron index

Excitatory connections to INs

Postsynaptic neuron index

	1	2	3	4	5
1	0	1	0	0	0
2	0	0	1	0	0
3	0	0	0	1	0
4	0	0	0	0	1
5	1	0	0	0	0

Presynaptic neuron index

Inhibitory connections to SCs

Postsynaptic neuron index

	1	2	3	4	5
1	2	1	1	1	0
2	0	2	1	1	1
3	1	0	2	1	1
4	1	1	0	2	1
5	1	1	1	0	2

Presynaptic neuron index

Excitatory connections to SCs

Postsynaptic neuron index

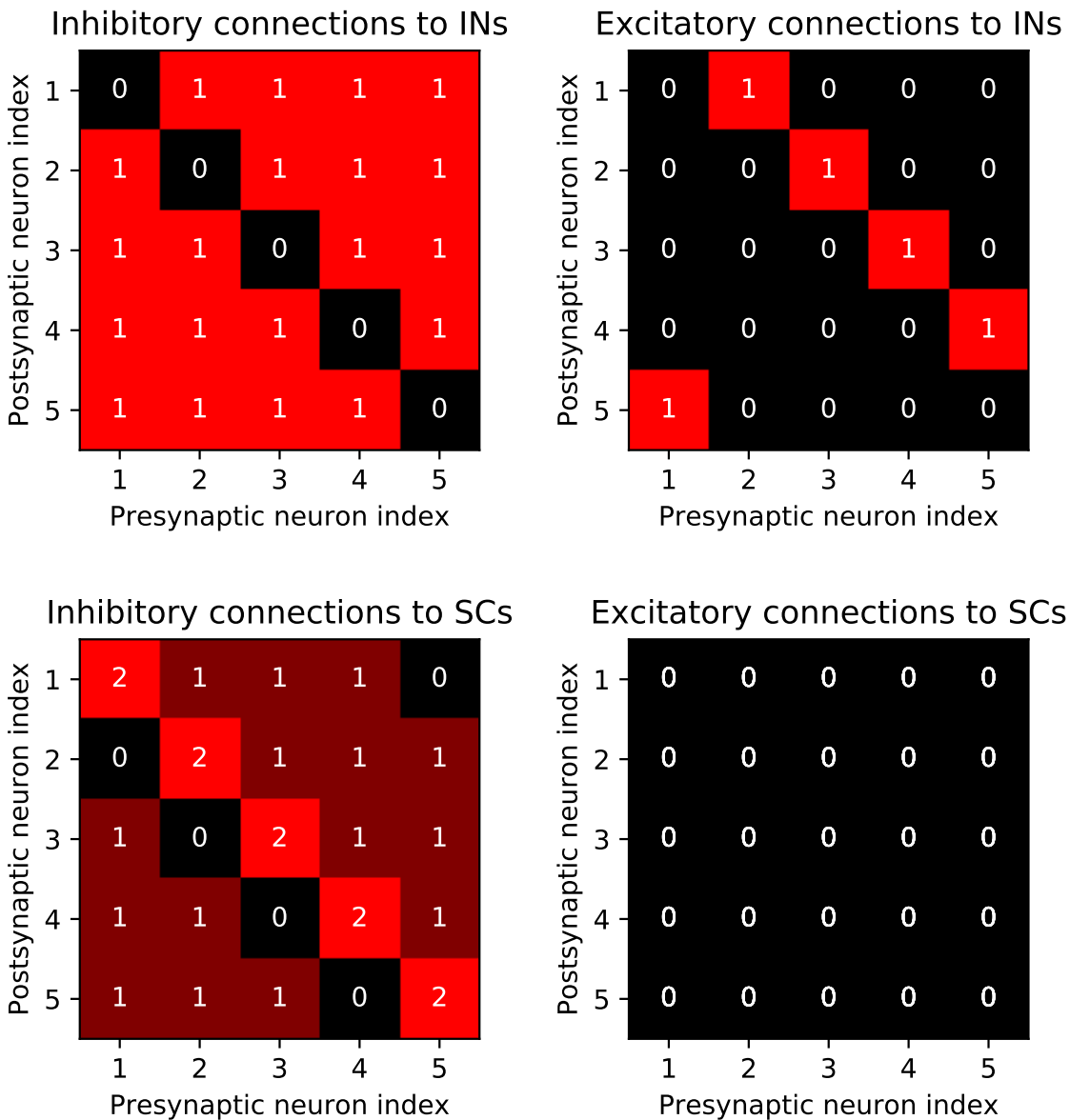|	1	2	3	4	5
1	0	0	0	0	0
2	0	0	0	0	0
3	0	0	0	0	0
4	0	0	0	0	0
5	0	0	0	0	0

Presynaptic neuron index

Figure 2.5: Connections in Network 2. Top panels: Connections to interneurons. Bottom panels: Connections to stellate cells. In each figure, the presynaptic neurons are indexed along the X axis and the postsynaptic neurons are indexed along the Y axis. The internal values represent the strength of synaptic connection, if any.

neurons participating in each one with different firing rates. In an effort to account for the former, the mechanism of formation of the bump and its translation was changed. Since we wanted stellate cells to spike multiple times, current was provided to stellate cells. However, exciting all the stellate cells in this manner would have made for

multiple stellate cells firing very close to each other temporally. To curb this, each interneuron was allowed to inhibit most stellate cells. Specifically, interneurons were not allowed to inhibit the stellate cell innervating them, but inhibited all others. This made sure that at any given point in time, only one stellate cell fired, along with the single interneuron that was excited by it.

Just like in the case of Network 1, this connectivity relies on the rebound-firing property of stellate cells to translate the bump. The difference is that the stellate cell next in the sequence of firing does not escape from inhibition immediately due to the inhibitory spikes arriving from the active interneuron. With each inhibitory spike, the membrane potential in the stellate cell rises a little, but is prevented from reaching the spiking threshold due to the arrival of an inhibitory spike. This process occurs multiple times, with the stellate cell's voltage reaching ever higher levels before it is inhibited. Eventually, the membrane potential does cross the spiking threshold, at which point it is able to fire. This firing activates a different interneuron and due to the global inhibition, silences the previously active one. The spiking of this new interneuron-stellate cell pair then starts to inhibit the next stellate cell in the sequence and the pattern proceeds thusly.

To be certain that the correct stellate cell escaped from inhibition, the synaptic weights from interneurons to stellate cells were tweaked. In Network 1, the connectivity matrix had values of 1 for inhibitory connections from interneurons to stellate cells. Both higher and lower values were tested to observe the behaviour of stellate cell rebound-spiking. Populating the synaptic weight matrix with appropriate values gave us bumps that were constituted of multiple spikes (connections shown in Figure 2.5).

2.4 Speed tuning

Because the grid cell network activity is correlated with the motion of the mouse, it was necessary that the speed of translation of the bump in our networks be tunable. In the two networks, speed tuning was achieved in different ways.
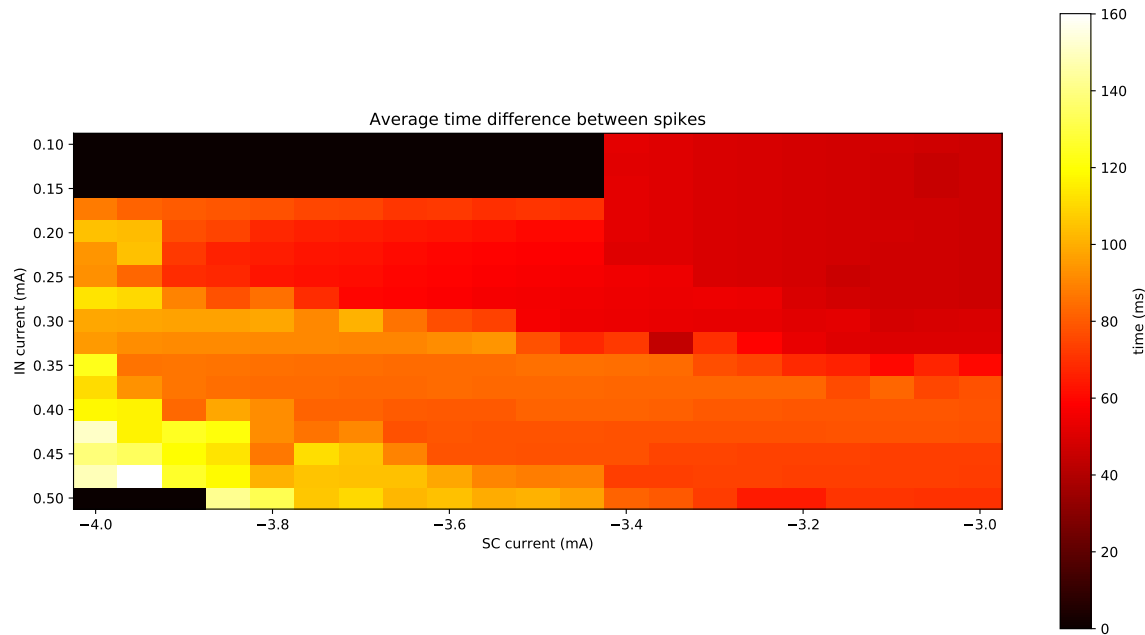
Figure 2.6: Speed tuning in Network 1, measured as average time elapsed between successive stellate cell spikes. The input current to SCs and the excited INs were varied while that to the inhibited INs was unchanged (-10 mA).

2.4.1   Speed tuning in Network 1

The activity bump in Network 1 was constituted of a single rebound-spike of a stellate cell which was able to spike between consecutive spikes of the interneuron inhibiting it. The timing of firing of the stellate cells depended both on the current input to stellate cells, as well as the frequency of firing of the interneurons (which was determined by the amplitude of current input to it). Thus, by varying the two current inputs, we reasoned that we would be able to change the speed of translation of the network. The effects of varying the two currents is shown in Figure 2.6.

2.4.2   Speed tuning in Network 2 – Theta oscillations

Using a ring of stellate cells and a corresponding ring of interneurons, we were able to produce a bump of activity that was also able to move. However, since stellate cells show strong rebound spiking, exciting them to drive the circuit (as is the case in Network 2) made the switching of the readout extrememly fast. This is unlike the case
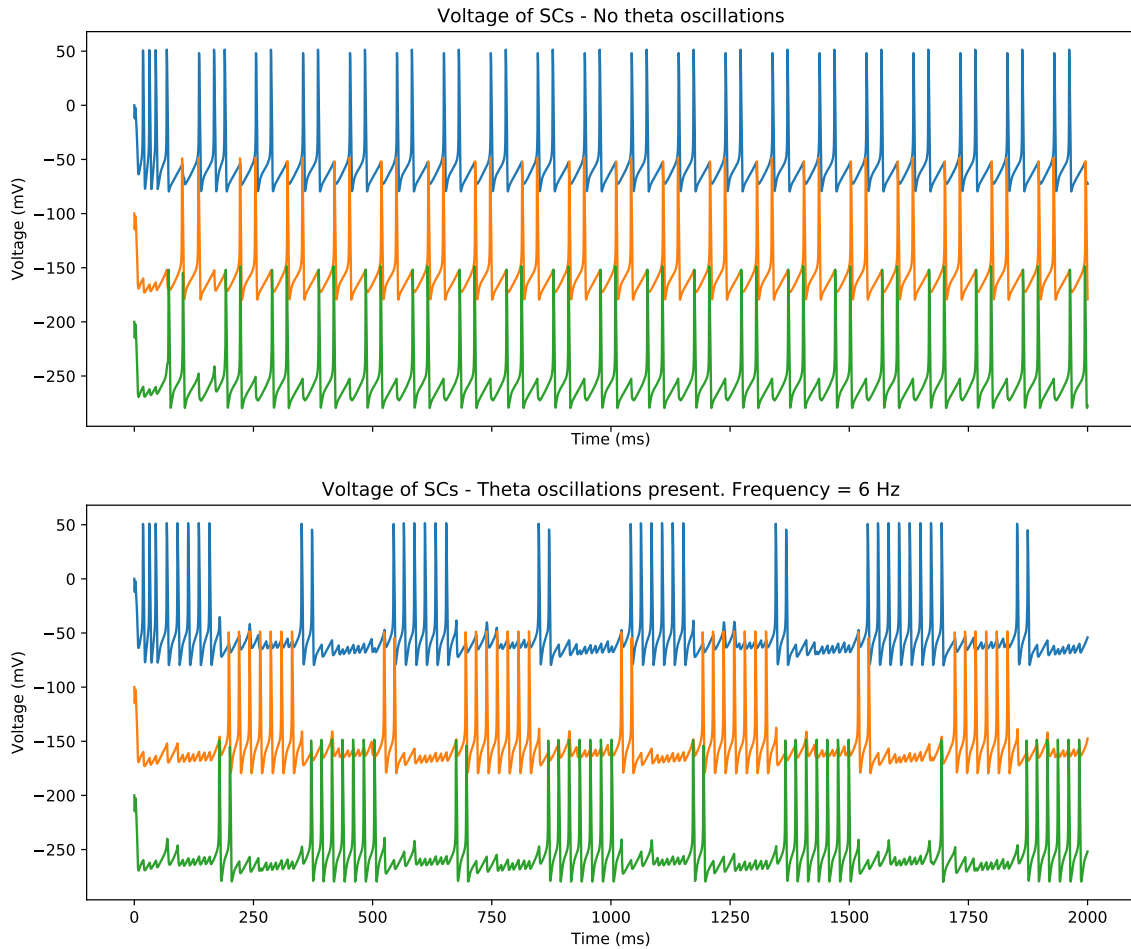
Figure 2.7: Tunability of Network 2 using theta oscillations. Top panel: Voltage traces of SCs in the absence of theta oscillations. Bottom panel: Voltage traces of SCs in the presence of theta oscillations, oscillation frequency = 6 Hz. Current values used: SC input = 1 mA, IN input = 0 mA.

of Network 1, and the speed of bump-translation cannot be controlled appreciably by simply varying the current input to cells. Such fast spiking can also lead to out-of-turn firing by stellate cells, a sufficient amount of which can lead to errors in translation of the bump. This is remedied to an extent by having differential synaptic strengths from interneurons to stellate cells. While each interneuron inhibits most stellate cells equally, if it inhibits a particular stellate cell more than the others, the stellate cell in question always is next in the sequence to show a burst of spikes. This behaviour is further made more robust by the addition of a theta oscillation (Figure 2.7). The theta rhythm or oscillation is an oscillation in the Mean Field Potential (MFP) of the

local environment of interneurons. It has a frequency between 6 and 12 Hz and has been observed to increase its frequency in accordance to the speed of motion of the mouse. Upon coupling the interneurons to theta oscillations, the robustness of the changing network activity increased and a large portion of the background spiking disappeared.
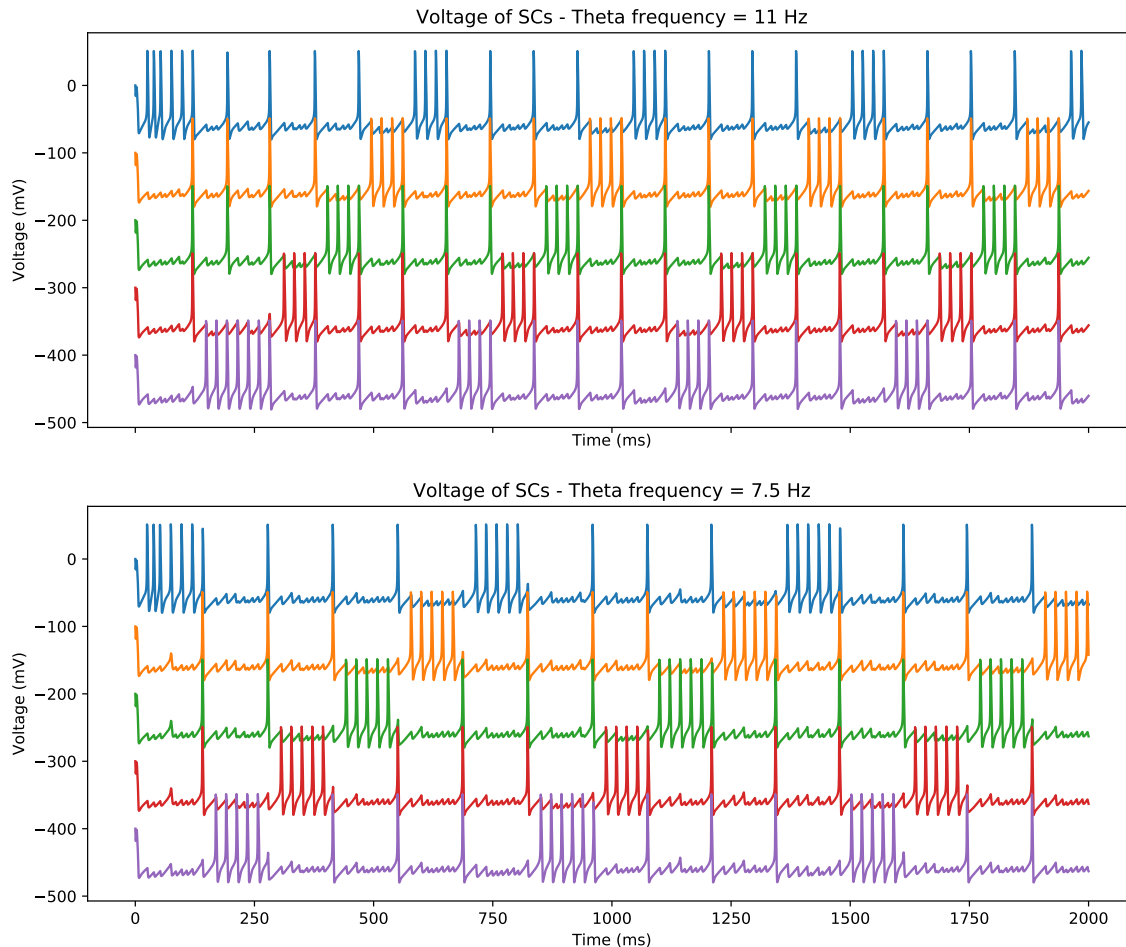

Figure 2.8: Speed tuning in Network 2. Both panels show voltage traces of SCs. Top panel: theta oscillation frequency = 11 Hz. Bottom panel: theta oscillation frequency = 7.5 Hz. Current values used are: SC input = 1 mA, IN input = 0 mA.

During the positive phase of the oscillation, the firing frequency of interneurons was lower than in the negative phase. This provided an opportunity for the stellate cells to show rebound-spiking, as any decrease in inhibition could cause stellate cells to do this. This is in fact the mechanism by which the network's activity locus

changes. Since the bump moved only when the theta drive was in a specific phase of its cycle, changing the frequency of the theta oscillation might have been sufficient to change the speed of translation of the bump. Indeed, we found that the switching followed the phase of theta at different frequencies of oscillation. Two cases are shown in Figure 2.8 where with a higher frequency of oscillation (11 Hz), the switching of stellate cell firing occured faster than in the case with a lower frequency (8 Hz).

Chapter 3

Discussion

3.1 Formation and movement of activity bump

Grid cells exhibit a wide variety of responses, of which the most basic is the existence of activity bumps and the ability to move them around. Our networks of stellate cells and interneurons have been able to showcase these behaviours by virtue of specific asymmetries in synaptic connections between neurons. This is a core idea behind continuous attractor networks which treat the activity of networks as the result of the interactions between its constituent members, as opposed to each cell being able to show these behaviours individually. Essentially, the population-level activity is an emergent phenomenon due only to asymmetries in connections. We have observed that varying not only the connections but also their synaptic strengths results in great variations in the activity of the network, which fits into the view that the connections between neurons are of paramount importance.

The fact that the grid cell activity persists, while being robust, in the absence of sensory cues leads one to conclude that the network is able to operate at least reasonably well with a reduced set of possible inputs. Of particular interest is the possibility that in such a scenario, place cells should not directly be involved in the formation of the grid-like patterns. Other types of inputs that would be active in such a scenario are idiothetic ones like speed and head-direction input. Some of these inputs have been simulated in our model using constant DC inputs.

3.1.1   Differential synaptic strengths in Network 2

In the case of Network 2, it was observed that stellate cells that are weakly inhibited escape from inhibition faster than ones that are more strongly inhibited (during the respective phase of the theta oscillation). Even so, we decided to strongly inhibit the next-in-sequence stellate cell (as compared to the others) so that it is the only one not firing immediately. A key observation that helped us in making this decision was that when a stellate cell fired, its status was essentially reset [Acker et al., 2003, Dickson et al., 2000]. This meant that the rebound-spiking behaviour of these cells was only fully reset once the cell has fired. In our model, after the other stellate cells fired and reset their state (as can be seen in Figures 2.7 and 2.8), the next-in-sequence cell was closer to its firing threshold than the others and so, went on to fire and show a burst of spikes.

3.2   Tuning the speed of the network

The mechanisms behind the formation and movement of the bumps in our two models, different as they are, are both primarily based on the rebound-spiking characteristics of stellate cells. Both models had interneurons that mediated which stellate cells showed rebound-spiking and when. In Network 1, the timing of firing of stellate cells was dependent on that of interneurons and so, by varying the current inputs to both, we were able to tune the speed of translation of the bump. Lower input to interneurons made them fire with greater delay, giving time to the stellate cells to escape from inhibition faster. Increasing the current input to the stellate cells made their membrane potential rise faster to their spiking threshold and subsequently escape from inhibition sooner. Both of these effects were seen in Figure 2.6, where the speed tuning of the network was measured by looking at the average time difference between successive spikes. The neurons were found to be extremely sensitive to the current input given to them. the range of current input for which grid cell-like activity was seen was 0.2 to 0.5 mA. Any higher and the stellate cells were unable to escape from their inhibition, and any lower made the interneurons unable to reach their firing threshold. In the case of current higher than 0.5 mA, the activity of the network is equivalent to the bistable switch regime of the primitive motif where

the active interneuron continually spikes until perturbed. Because the ratio of the number of stellate cell spikes to those of interneurons underwent a change at particular values of current, discontinuities can be seen in the speed tuning. However, except in these cases, the speed tuning in Network 1 followed the variation in input current as expected: higher stellate cell input and lower interneuron input resulted in faster translation of the activity bump.

3.2.1 The role of theta oscillations in Network 2

With the specific connections in Network 2, combined with the presence of theta oscillations, we saw that the translation of the bump across neurons could indeed be restricted to certain phases of the theta drive. This allowed for stellate cells to escape from inhibition only during those periods. Speed tuning was then achieved by varying the periodicity of these windows by changing the frequency of the theta drive. Unlike in the case of varying current input, this method provided a more continuous tunability of the system.

This fits well with the observation that the frequency of the theta oscillation follows the speed of motion of the mouse and by extension, is correlated to the activity of the grid cell network. While our results are not entirely indicative of theta being the agent responsible for making the temporal profile of firing more stable, it certainly added to the tunability of the model. Previous work in the lab has also shown that the theta drive could be responsible, at least in part, to gating information temporally across different regions of the brain. In this light, we did not consider the possible effects of theta on the inputs to our model. It is quite possible and even likely that by coupling the theta drive to the various inputs of our system, our model of the network will be able to show its behaviour in a more robust fashion.

3.3 Extension of the model

The networks that are presented in this study, while showing some characteristics of the grid cell network, do not capture the full picture. The biggest shortcomings are:

3.3.1 Unrealistic activity bumps

The activity bumps exhibited by grid cells comprise multiple neurons showing different firing rates. The bumps present in our models are idealizations of these bumps. The presented networks are able to demonstrate the movement of bumps, an integral characteristic of the grid cell network, however, neither of them represents the full picture even as far as the structure of the bump goes.

The activity bump of the grid cell network consists of multiple stellate cells firing at different rates. The cells at the center of each bump fire the fastest while cells towards its periphery fire slower. In contrast, our networks look more like delta functions: Network 1 showed only one spike per bump, and Network 2 showed multiple spikes but only from one cell.

3.3.2 Multiple bumps

The presence of multiple bumps is essential to a full model of the grid cell network. One way to incorporate these, even in the 1 dimension case, is by considering the use of local inhibition. Essentially, instead of inhibiting all stellate cells and interneurons, each interneuron can inhibit cells in a more local environment around it. Neurons, particularly interneurons, that are outside the zone of inhibition would be free to fire. This would result in multiple interneurons firing simultaneously in different regions, leading to the formation and movement of multiple bumps along the line of neurons.

3.3.3 Network activity in 2 dimensions

The presented networks model the system's behaviour in a single spatial dimension. Extension of the model to the second dimension is not trivial as activity bumps need to be able to traverse the sheet of neurons across any direction. Previous work on the system has employed the use of direction input to grid cells which themselves show direction preference. Using our model as a motif, something similar might be possible by introducing direction preference to interneurons in a manner similar to how direction is selected for in the current Network 1.

Chapter 4

Conclusions

To simulate the activity of the grid cell network along a single dimension, we have employed the use of stellate cells and inhibitory interneurons to construct two networks that satisfactorily demonstrate the ability to form and translate an activity bump. These networks were based on the primitive circuit motif thought to be present in the MEC. We have also demonstrated the activity profiles of the motif. Our Network 1 was able to show direction-tuning by exciting and inhibiting entire sets of interneurons, and speed-tuning by varying the current inputs to the stellate cells and interneurons. With Network 2, we were able to make the activity bump more realistic while also incorporating the action of theta oscillations into the network. Network 2 was able to show speed-tuning as a function of the frequency of the theta drive.

The bumps that were obtained can be made even more realistic. Instead of a bump being comprised of a single cell's activity (like it is in our networks), bumps in the grid cell network are constituted of the activity of multiple cells firing at different frequencies. The number of bumps in our model is only one while the system has multiple bumps arranged in at regular intervals (in a single dimension). We think the latter can be achieved by implementing the use of local inhibitory fields of interneurons instead of the global inhibitory fields. Finally, our model needs to be extended to be able to represent motion in two spatial dimensions as opposed to the one that it can do at present. In two spatial dimensions, the arrangement of bumps will need to be along a hexagonal grid. These bumps would possibly remain stable and robust using local

inhibition by interneurons, and will be able to move by introducing direction-based inputs and specifities.

The activity of the cells was dictated by and large by the connections existing between them. Even small variations in these connections lead to qualitatively different types of activity shown by the population. Since there are many regimes of the parameters that have not been visited by us, more work is required to be able to characterize all of the behaviours of this system.

We hope that the networks presented in this thesis, though far from complete models of grid cells, will be instrumental in the creation of fuller and better models of this neuronal population.

Chapter 5

Materials and Methods

Our model uses two types of cells, stellate cells and interneurons.

5.1 Neuron Models

All neurons were modelled as conductance-based, single-compartment spiking neuron models. The ionic conductance for ion x was modelled as:

$$I_x = g_x(V, t)(V - E_x)$$

where $g_x(V, t)$ is the conductance of channels and E_x is the reversal potential for that ion. $g_x(V, t)$ is specified in terms of the maximal conductance g_x and the state of the gating variables. Each gating variable followed first-order kinetics and were modelled as follows (for gating variable m):

$$\frac{dm}{dt} = -\frac{(m - m_\infty)}{\tau_m}$$

where m_∞ and τ_m are functions of voltage. An equivalent form of the above equation is:

$$\frac{dm}{dt} = \alpha_m(1 - m) - \beta_m m$$

where $m_\infty = \alpha_m/(\alpha_m + \beta_m)$ and $\tau_m = 1/(\alpha_m + \beta_m)$

5.1.1   Stellate cells

The equation describing stellate cell behaviour [Acker et al., 2003] is:

$$C\frac{dV}{dt} = I_{ext} - I_{Na} - I_K - I_L - I_h - I_{NaP} - I_{syn}$$

This model of stellate cells involves the standard I_{Na}, I_K, and I_L conductances in addition to a hyperpolarization-activated depolarizing current (I_h), and a persistent sodium current (I_{NaP}). The presence of both conductances is necessary to see both sub-threshold oscillations and rebound-spiking dynamics [Acker et al., 2003, Dickson et al., 2000]. The equations describing ionic conductances and parameters for stellate cells are given in Table 5.1.

5.1.2   Interneurons

The dynamics of interneurons [Wang and Buzsaki, 1996] was modelled using the equation:

$$C\frac{dV}{dt} = I_{ext} - I_{Na} - I_K - I_L - I_{syn} - I_\theta$$

Since these interneurons are able to show rapid spiking, the state of the gating variable m was taken to be that at $t = \infty$, i.e., $m(t) = m_\infty$. The equations describing ionic conductances and parameters for interneurons are given in Table 5.2.

5.2   Synapse Models

Synaptic currents were modelled as follows:

$$I_{syn} = g_{syn}s(V_{post} - E_{syn})$$

$$\frac{ds}{dt} = F(V_{pre})\alpha_s(1 - s) - \beta_s$$

where g_{syn} is the maximal synaptic conductance, s is a gating variable, $F(V_{pre}) = \frac{1}{2}(1 + tanh(V_{pre}/4))$ models the opening of a synaptic ion channel in response to an

action potential in the presynaptic neuron, and E_{syn} is the reversal potential, the value of which, determined whether the synapse was excitatory or inhibitory. The values of the various parameters used are given below.

5.2.1 Synaptic parameters - Network 1

The synaptic parameters used in Network 1 were: $E_{exc} = 0.0$, $E_{inh} = -80.0$, $g_{ei} = 0.3$, $g_{es} = 0.0$, $g_{ii} = 1.0$, $g_{is} = 0.6$, $\alpha_i = 3.33$, $\beta_i = 0.11$, $\alpha_e = 100.0$, $\beta_e = 0.33$
where g_{ei} is used for excitatory connections to interneurons, g_{es} is used for excitatory connections to stellate cells, g_{ii} is used for inhibitory connections to interneurons, and g_{is} is used for inhibitory connections to stellate cells.

5.2.2 Synaptic parameters - Network 2

The synaptic parameters used in Network 2 were: $E_{exc} = 0.0$, $E_{inh} = -80.0$, $g_{ei} = 0.5$, $g_{es} = 0.0$, $g_{ii} = 1.0$, $g_{is} = 0.6$, $\alpha_i = 3.33$, $\beta_i = 0.11$, $\alpha_e = 100.0$, $\beta_e = 0.33$
where g_{ei} is used for excitatory connections to interneurons, g_{es} is used for excitatory connections to stellate cells, g_{ii} is used for inhibitory connections to interneurons, and g_{is} is used for inhibitory connections to stellate cells.

5.3 Input to the system

Two types of input were given to the system. These are the contant DC input, and the theta oscillation. The former was provided to all cells while the latter was only given to the interneurons.

5.3.1 Constant DC

DC input was given to neurons which were meant to simulate inputs from neurons upstream to the system. This ranged from currents of different strengths applied to

neurons at different times, to currents of equal strengths given to multiple neurons of the same type at the same time. Broadly, the profile of this kind of input specified the 'state' of the system.

5.3.2   Theta oscillation

The other kind of input was the theta rhythm. Theta current was modelled as a sinusoid in the following way:

$$I_\theta = A\sin(2\pi\omega t + \phi)(V - V_{th})$$

where $A = 0.2$ is the amplitude of the theta oscillation, ω is its frequency in Hz, and $V_{th} = -80$ mV is the threshold voltage.

5.4   Connectivity

A number of different connectivty profiles were used throughout the duration of the project. The initial motif [Neru and Assisi, 2019] consisted of two stellate cells and two interneurons. Another motif used was the stellate cell driven motif in Network 2. Multiple simulations were run to arrive at the synaptic strengths that provided the most robust activity profiles in terms of reliability and sequential firing. The connection matrices for Network 1 and Network 2 are given in Figure 5.1 and Figure 5.2 respectively.

5.5   Tensorflow

All simulations were run using Tensorflow, Version 1.13.1 using the methods described in [Mohanta and Assisi, 2019]. The Euler method was used to perform integrations and the time interval of integration was set to $dt = 0.01$ ms.

Conductance type	Equations	Parameters
Na	$I_{Na} = g_{Na}m^3h(V - E_{Na})$ $\alpha_m = -0.1(V + 23)/(e^{-0.1(V+23)} - 1)$ $\beta_m = 4e^{-(V+48)/18}$ $\alpha_h = 0.07e^{-(V+37)/20}$ $\beta_h = 1/(e^{-0.1(V+7)} + 1)$	g_{Na}= 52.0 $E_{Na} = 55.0$
K	$I_K = g_K n^4(V - E_K)$ $\alpha_n = -0.01(V + 27)/(e^{-0.1(V+27)} - 1)$ $\beta_n = 0.125e^{-(V+37)/80}$	$g_K = 11.0$ $E_K = -90.0$
NaP	$I_{NaP} = g_{NaP}ms(V - E_{Na})$ $ms_\infty = 1/(1 + e^{-(V+38)/6.5})$ $t_{ms} = 0.15$	$g_{NaP} = 0.5$
HCN	$I_h = g_h(0.65mhf + 0.35mhs)(V - E_h)$ $mhf_\infty = 1/(1 + e^{(V+79.2)/9.78})$ $t_{mhf} = 1 + 0.51/(e^{(V-1.7)/10} + e^{-(V+340)/52})$ $mhs_\infty = 1/(1 + e^{(V+2.83)/15.9})^{58}$ $t_{mhs} = 1 + 5.6/(e^{(V-1.7)/14} + e^{-(V+260)/43})$	$g_h = 1.5$ $E_h = -20.0$
Leak	$g_L(V - E_L)$	$g_L = 0.5$ $E_L = -65.0$

Table 5.1: Equations and parameters for stellate cell conductances

Conductance type	Equations	Parameters
Na	$I_{Na} = g_{Na}m^3h(V - E_{Na})$ $\alpha_m = -0.1(V + 35)/(e^{-0.1(V+35)} - 1)$ $\beta_m = 4e^{-(V+60)/18}$ $\alpha_h = 0.07e^{-(V+58)/20}$ $\beta_h = 1/(e^{-0.1(V+28)} + 1)$	$g_{Na} = 35.0$ $E_{Na} = 55.0$
K	$I_K = g_K n^4(V - E_K)$ $\alpha_n = -0.01(V + 34)/(e^{-0.1(V+34)} - 1)$ $\beta_n = 0.125e^{-(V+44)/80}$	$g_K = 9.0$ $E_K = $ -90.0
Leak	$g_L(V - E_L)$	$g_L = 0.1$ $E_L = $ -65.0

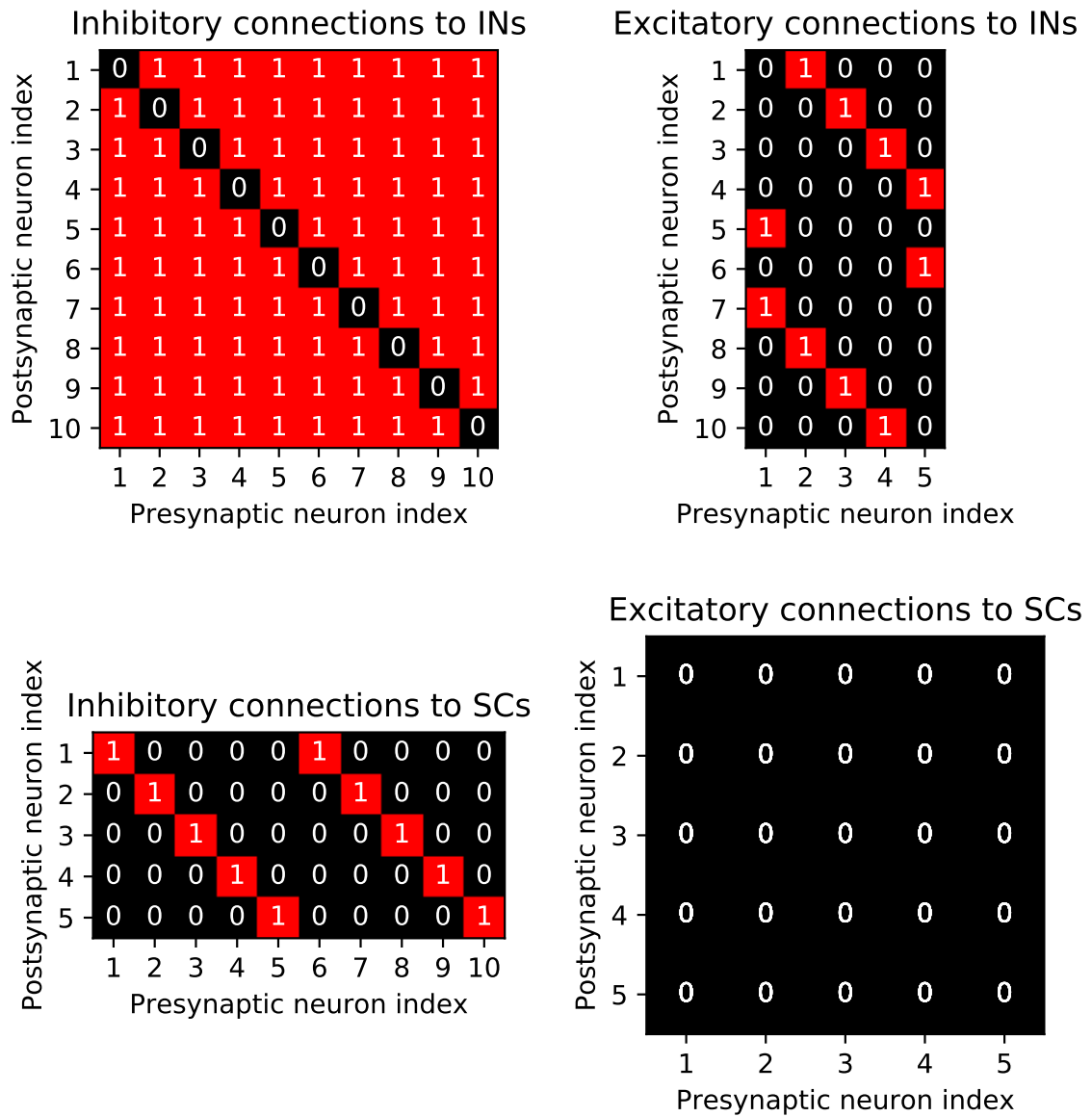Table 5.2: Equations and parameters for interneuron conductances

Figure 5.1: Connections in Network 1. Top panels: Connections to interneurons. Bottom panels: Connections to stellate cells. In each figure, the presynaptic neurons are indexed along the X axis and the postsynaptic neurons are indexed along the Y axis. The internal values represent the strength of synaptic connection, if any.
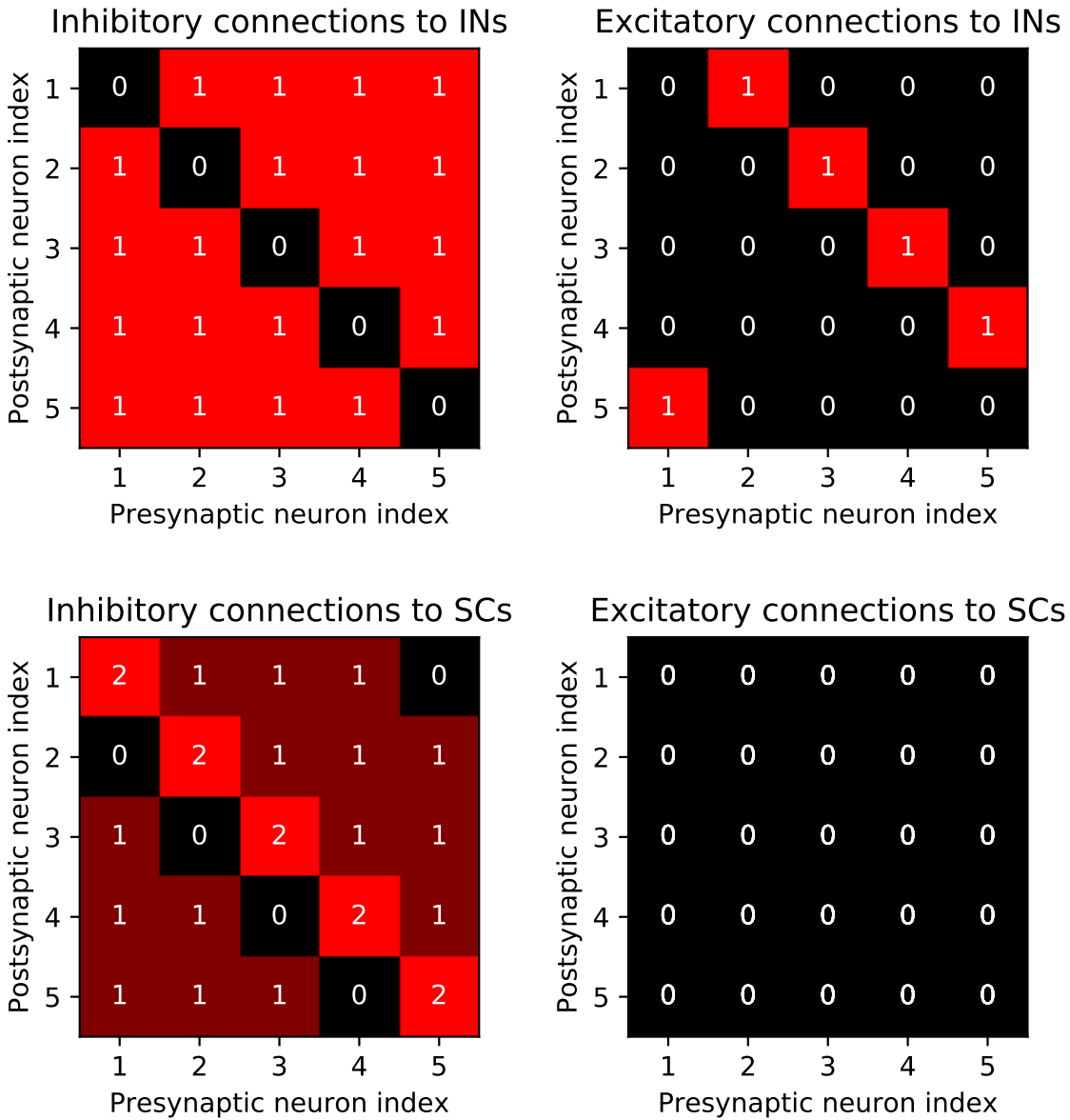
Figure 5.2: Connections in Network 2. Top panels: Connections to interneurons. Bottom panels: Connections to stellate cells. In each figure, the presynaptic neurons are indexed along the X axis and the postsynaptic neurons are indexed along the Y axis. The internal values represent the strength of synaptic connection, if any.

Bibliography

[Acker et al., 2003] Acker, C.D., Kopell, N., and White, J.A. (2003). Synchronization of strongly coupled excitatory neurons: Relating network behaviour to biophysics. *Journal of Computational Neuroscience*, **15**(1):71-90.

[Alonso and Llinas, 1989] Alonso, A., and Llinas, R.R. (1989). Subthreshold Na^+-dependent theta-like rhythmicity in stellate cells of entorhinal cortex layer II. *Nature*, **342**:175-177

[Alonso and Klink, 1993] Alonso, A. and Klink, R. (1993). Differential electroresponsiveness of stellate and pyramidal-like cells of medial entorhinal cortex layer II. *Journal of Neurophysiology*, **70**(1):128-143.

[Burak and Fiete, 2009] Burak, Y. and Fiete, I. R. (2009). Accurate path integration in continuous attractor network models of grid cells. *PLoS Computational Biology*, **5**(2):e1000291.

[Dickson et al., 2000] Dickson, C.T., Magistretti, J., Shalinsky, M.H., Fransén, E., Hasselmo, M.E., and Alonso, A. (2000). Properties and role of I(h) in the pacing of subthreshold oscillations in entorhinal cortex layer II neurons. *Journal of Neurophysiology*, **83**(5):2562-2579.

[Giocomo et al., 2011] Giocomo, L.M., Moser, M.-B., and Moser, E.I. (2011). Computational models of grid cells. *Neuron*, **71**(4):589-603.

[Hafting et al., 2005] Hafting, T., Fyhn, M., Molden, S., Moser, E.I & Moser, M.-B. (2005). Microstructure of a spatial map in the entorhinal cortex. *Nature*, **436**(7052):801-806

[Neru and Assisi, 2019] Neru, A., and Assisi, C. (2019). Theta oscillations gate the transmission of reliable sequences in the medial entorhinal cortex. doi: https://doi.org/10.1101/545822

[McNaughton et al., 1996] McNaughton, B. L., Barnes, C. A., Gerrard, J. L., Gothard, K., Jung, M. W., Knierim, J. J., Kudrimoti, H., Qin, Y., Skaggs, W.

E., Suster, M., and Weaver, K. L. (1996). Deciphering the hippocampal polyglot: the hippocampus as a path integration system. *Journal of Experimental Biology*, **199**(1):173-185.

[McNaughton et al., 2006] McNaughton, B. L., Battaglia, F. P., Jensen, O., Moser, E.I., and Moser, M.-B. (2006). Path integration and the neural basis of the cognitive map. *Nature Reviews Neuroscience*, **7**(8):663-678.

[Mohanta and Assisi, 2019] Mohanta, S.S., and Assisi,C. (2019). Parallel scalable simulations of biological neural networks using TensorFlow: A beginner's guide. doi:arXiv:1906.03958

[O'Keefe, 1976] O'Keefe, J. (1976). Place units in the hippocampus of the freely moving rat. *Experimental Neurology*, **51**(1):78-109.

[Sargolini et al., 2006] Sargolini, F., Fyhn, M., Hafting, T., McNaughton, B. L., Witter, M. P., Moser, M.-B., and Moser, E. I. (2006). Conjunctive representation of position, direction, and velocity in entorhinal cortex. *Science*, **312**(5774):758-762.

[Wang and Buzsaki, 1996] Wang, X.-J, and Buzsaki, G. (1996). Gamma oscillation by synaptic inhibition in a hippocampal interneuronal network model. *Journal of Neuroscience*, **16**(20):6402-6413.

[Zilli, 2012] Zilli, E. A. (2012). Models of grid cell spatial firing published 2005-2011. *Frontiers in Neural Circuits*, **6**.